PCCP

PAPER

View Article Online
View Journal | View Issue

Cite this: *Phys. Chem. Chem. Phys.*, 2015, **17**, 13307

Highly active electrolytes for rechargeable Mg batteries based on a $[Mg_2(\mu\text{-}Cl)_2]^{2+}$ cation complex in dimethoxyethane†

Yingwen Cheng,[a] Ryan M. Stolley,[b] Kee Sung Han,[c] Yuyan Shao,[a] Bruce W. Arey,[c] Nancy M. Washton,[c] Karl T. Mueller,[cd] Monte L. Helm,[b] Vincent L. Sprenkle,[a] Jun Liu[a] and Guosheng Li*[a]

Received 10th February 2015,
Accepted 13th April 2015

DOI: 10.1039/c5cp00859j

www.rsc.org/pccp

A novel $[Mg_2(\mu\text{-}Cl)_2]^{2+}$ cation complex, which is highly active for reversible Mg electrodeposition, was identified for the first time in this work. This complex was found to be present in electrolytes formulated in dimethoxyethane (DME) through dehalodimerization of non-nucleophilic $MgCl_2$ by reacting with either Mg salts (such as $Mg(TFSI)_2$, TFSI = bis(trifluoromethane)sulfonylimide) or Lewis acid salts (such as $AlEtCl_2$ or $AlCl_3$). The molecular structure of the cation complex was characterized by single crystal X-ray diffraction, Raman spectroscopy and NMR. The electrolyte synthesis process was studied and rational approaches for formulating highly active electrolytes were proposed. Through control of the anions, electrolytes with an efficiency close to 100%, a wide electrochemical window (up to 3.5 V) and a high ionic conductivity (>6 mS cm^{-1}) were obtained. The understanding of electrolyte synthesis in DME developed in this work could bring significant opportunities for the rational formulation of electrolytes of the general formula $[Mg_2(\mu\text{-}Cl)_2][anion]_x$ for practical Mg batteries.

Introduction

Magnesium (Mg)-based rechargeable batteries have recently emerged as attractive candidates for next generation energy storage devices due to the unique advantages of Mg metals.[1–3] Mg is an earth abundant and environmentally benign material and is safe to handle when used as an anode, and has a low standard electrode potential and fast deposition/stripping kinetics without the formation of dendritic structures.[4] Over the past few decades, significant progresses have been made in the quest for rechargeable Mg batteries, including the development of cathode materials,[1,5–8] electrolytes,[9–15] current collectors[16–18] and anode materials.[19–21] The commercialization of Mg batteries, however, has not yet been demonstrated and still faces great challenges. Substantial advances, particularly, in the development of stable/safe electrolytes with wide electrochemical windows and on high voltage cathode materials with high capacity, are critically required.

The electrolyte is one key component for rechargeable batteries.[22,23] It provides electrochemically active species and determines the electrode–electrolyte interfaces both for cathodic and anodic electrochemical reactions, and therefore, plays pivotal roles in determining battery performance. The importance of the electrolyte for Mg battery development is particularly significant and it is currently a major limiting factor for its practical applications.[11] Simple battery electrolytes prepared by dissolving Mg salts, such as $Mg(ClO_4)_2$, in aprotic solvents are usually not able to produce reversible Mg deposition, most likely due to the formation of blocking layers.[24]

During the past few decades, there has been an increase in studies for formulating electrolytes capable of reversible Mg deposition.[2,11,25,26] Gregory *et al.* initially developed ethereal solutions containing Mg organo-aluminates or Mg organo-borates and examined their activities for Mg deposition.[27] Aurbach *et al.* later demonstrated electrolytes with an anodic stability of ~2.5 V through reacting Grignard reagents (MgR_2, R = ethyl and butyl) with aluminum containing Lewis acids ($AlEtCl_2$ or $AlCl_3$) and established the first prototypes of rechargeable Mg batteries.[1] Since then this type of electrolyte has been intensively studied and its properties were further optimized using the same concept through suitable combinations

[a] *Energy Processes & Materials Division, Energy and Environmental Directorate, Richland, WA 99352, USA. E-mail: guosheng.li@pnnl.gov*
[b] *Catalysis Science Division, Fundamental & Computational Science Directorate, Richland, WA 99352, USA*
[c] *Environmental Molecular Science Laboratory, Pacific Northwest National Laboratory, Richland, WA 99352, USA*
[d] *Department of Chemistry, Pennsylvania State University, University Park, PA 16082, USA*

† Electronic supplementary information (ESI) available: Detailed synthesis methods, full details of single crystal X-ray structure refinement and additional supporting figures. See DOI: 10.1039/c5cp00859j

of different Mg Grignard reagents and Lewis acid compounds.[28] For example, Pour *et al.* used phenyl magnesium chloride and synthesized all-phenyl-complex (APC) electrolytes that have electrochemical windows exceeding 3.3 V.[10,29] Because of the inherent safety concerns related to Grignard reagents, other Mg compounds such as $MgCl_2$,[13–15] ROMgCl,[30] hexamethyldisilazide magnesium chloride (HDMSMgCl),[31] and magnesium bistrifluoromethane sulfonyl imide ($Mg[TFSI]_2$)[32,33] were recently used to formulate electrolytes. Interestingly, crystallographic studies suggest that the cation complex unit $[Mg_2(\mu\text{-}Cl)_3]^+$ was commonly observed in almost all of the salts crystallized from electrochemically active magnesium organohaloaluminate and magnesium organoborate electrolytes in tetrahydrofuran (THF) solution. This cation complex consisted of two octahedrally coordinated Mg atoms bridged by three chloride atoms and paired with a counter anion.[12,13,34] It should be noted, however, that in solution this complex might be in thermodynamic equilibrium with THF-solvated $MgCl_2/MgCl^+$ species and therefore the actual composition of the electrolyte is rather complicated.[11,14] Compared with these THF-based electrolytes that have been studied relatively well, formulation of electrolytes in other ethereal solvents (such as DME and diglyme) has been studied to a far lesser extent. The successful demonstration and fundamental understanding of the synthesis of electrolytes in solvents with better thermal and chemical stability than THF are critical for future improvements of feasible rechargeable Mg batteries.

In this paper we report the first identification and analysis of a unique active cation complex $[Mg_2(\mu\text{-}Cl)_2(DME)_4]^{2+}$ for reversible Mg deposition and discuss factors that could affect its activity. This complex was found to be present in a series of electrolytes formulated in DME by dehalodimerization of $MgCl_2$ through reacting with either Mg salts ($Mg(TFSI)_2$) or Lewis acid salts ($AlEtCl_2$ or $AlCl_3$) and the approach could be extended to other salt combinations. The chemical structure was studied and confirmed by single crystal X-ray diffraction (XRD), Raman spectroscopy and ^{25}Mg and ^{27}Al nuclear magnetic resonance (NMR). Furthermore, it was found that through the control of anion chemistry (both the type and the concentration), electrolytes with a coulombic efficiency close to 100%, a high anodic stability ($\sim$3.5 V), and a high ionic conductivity ($\sim$6 mS cm^{-1}) could be obtained readily. Our results suggest that solvent molecules play critical roles in determining the structure of active Mg species and strongly affect their activity for Mg deposition. The electrolyte synthesis and understanding developed in this work could be insightful for rational formulation of a family of electrolytes of the general formula $[Mg_2(\mu\text{-}Cl)_2(DME)_4][anion]_x$, and provide new opportunities for developing cathode materials, and therefore could be significant for practical Mg batteries.

Results and discussion

Our previous work demonstrated synthesis of active Mg electrolytes by reacting $MgCl_2$ with Lewis acids in THF.[13] The use of THF, however, could be problematic for practical applications because it has low boiling point (66 °C) and flash point (−14 °C).

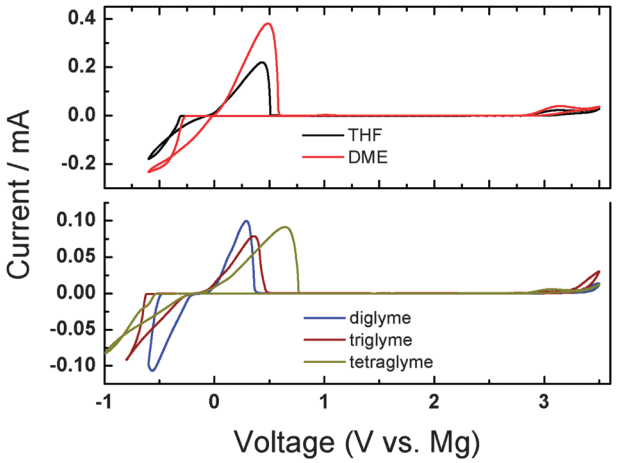

Fig. 1 CVs (2nd cycle) of Mg electrolytes synthesized by reacting 0.4 M $MgCl_2$ with a desired amount of $AlEtCl_2$ (see Table 1 for details) in different solvents as indicated. Note that all of these electrolytes were able to produce reversible Mg deposition and stripping. The electrochemical properties of these electrolytes are summarized in Table 1.

These intrinsic properties of THF have motivated us to study the formulation of Mg electrolytes in ethereal solutions with better thermal and chemical stability. To do this, we started with synthesis of electrolyte solutions in DME, diglyme, triglyme and tetraglyme using identical concentrations of precursors (0.4 M $MgCl_2$ and 0.4 M $AlEtCl_2$). The reaction products, without any purification, were directly used to examine their activity for Mg plating and stripping. Fig. 1 shows a set of CVs recorded from these solutions at 20 mV s^{-1} on a Pt working electrode and Table 1 provides a comparison of their electrochemical activities (Mg deposition overpotential and coulombic efficiency) and ionic conductivities. The behavior of typical $MgCl_2$–$AlEtCl_2$/THF electrolytes was also provided for reference.[13] It was found that all of these electrolytes were able to produce reversible Mg deposition and stripping and they exhibited similar anodic stability. A small irreversible oxidization peak at *ca.* $\sim$2.9 V *vs.* Mg, presumably due to reactions of $AlEtCl_4^-$ anions, was observed for all these electrolytes and is limiting the anodic stability.[13] However, it should be noted that the anodic stability could be extended through optimization of anion chemistry using approaches, for example, that have been established for THF-based electrolytes.[14,15] More importantly, these electrolyte solutions showed pronounced solvent dependent electroactivity for Mg deposition (Table 1), likely due to the differences in solvent Mg ion complex structures with chloride ions and different solvent molecules, which in turn show different physicochemical properties in solvents, such as mobility, chemical stability and reactivity. Overall, the comparison implies that the electrolyte formulated in DME has beneficial properties for Mg deposition and has a high cycling efficiency (at least 95%, stable), a high ionic conductivity (4.10 mS cm^{-1}), a low Mg deposition overpotential (220 mV) and high Mg deposition current density (Fig. 1). The high ionic conductivity is similar to the well-established all-phenyl-complexes based electrolytes.[26] Therefore, all further experiments in this work were focused on this electrolyte system,

Table 1 Electrochemical properties of electrolytes synthesized using 0.4 M $MgCl_2$ and the desired amount of $AlEtCl_2$ in different solvents as indicated. These data were obtained based on CV experiments with Pt working electrodes (1 mm) at 20 mV s^{-1}

Solvent	Overpotential for Mg deposition (mV)	Coulombic efficiency (%)	Ionic conductivity (mS cm^{-1})
3 : 2 $MgCl_2$–$AlEtCl_2$/THF	252	95	2.09
1 : 1 $MgCl_2$–$AlEtCl_2$/DME	220	95	4.10
1 : 1 $MgCl_2$–$AlEtCl_2$/diglyme	404	81	2.29
1 : 1 $MgCl_2$–$AlEtCl_2$/triglyme	466	86	1.19
1 : 1 $MgCl_2$–$AlEtCl_2$/tetraglyme	384	84	0.95

but it should be noted that the properties of electrolytes synthesized in other long-chain glymes are also encouraging and worth further investigation.

The outstanding activity for electrolytes synthesized in DME is particularly attractive and was therefore further studied. The structure of the active species presented in this electrolyte was first analyzed using single crystal X-ray diffraction. Solid crystals were prepared by layering hexane on the top of 3 ml $MgCl_2$–$AlEtCl_2$/DME electrolyte and were identified as having the ionic pair of $[Mg_2(\mu\text{-}Cl)_2(DME)_4][AlEtCl_3]_2$ (Fig. 2a and Tables S1–S6, ESI†). The cation complex consists of two octahedrally coordinated Mg centers bridged by two chlorine atoms. The four remaining sites on each Mg atom are coordinated through the oxygen atoms provided by two DME molecules. The anion is an aluminum atom tetrahedrally coordinated by one ethyl group and three chlorine atoms. This complex has a fundamentally different molecular structure compared to the $[Mg_2(\mu\text{-}Cl)_3(THF)_6]^+$ complex observed in the THF-based electrolyte,[2,13] and could provide new opportunities for rational formulation of Mg electrolytes. In addition to the $MgCl_2$–$AlEtCl_2$ combination, we also confirmed that electrolytes synthesized in DME using $MgCl_2$–$AlCl_3$ and $MgCl_2$–$Mg(TFSI)_2$ also have the same cation species (Fig. 2b and Tables S7–S12, ESI,† and discussions below). We note that recent studies reported the synthesis of electrolytes in DME using similar formulae, $MgCl_2/AlCl_3$ and $MgCl_2/Mg(TFSI)_2$, but the structure of the active species was not identified,[15,32] and this study represents the first identification of this active species.

The composition of solid crystals suggests that the possible reaction involved in the synthesis of electrolytes is $MgCl_2$ + $AlEtCl_2$ → $[Mg_2(\mu\text{-}Cl)_2(DME)_4][AlEtCl_3]_2$ in DME. To gain more insight into this reaction, we synthesized and analyzed a series of solutions using 0.4 M $MgCl_2$ and varied concentrations of $AlEtCl_2$. It should be noted that the stoichiometry of the proposed reaction suggests that 0.4 M of $AlEtCl_2$ is required for complete reaction. All of the as-synthesized electrolytes were transparent and have no precipitates, and were directly used for electrochemical studies. Fig. 3 shows a set of CVs obtained

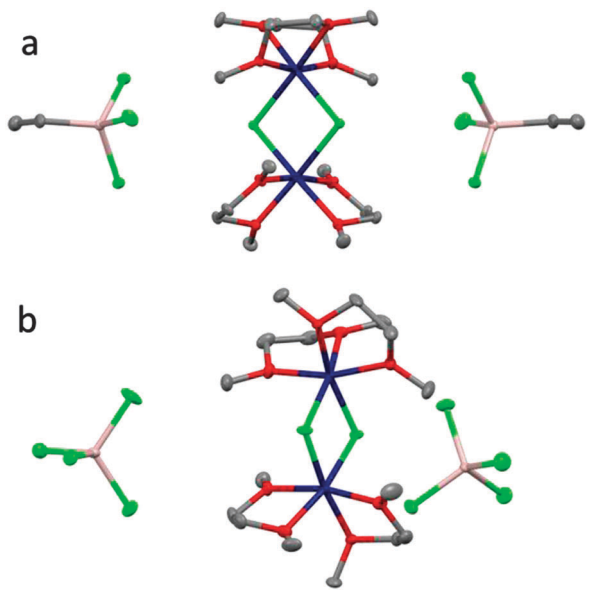

Fig. 2 Molecular structures of (a) $[Mg_2(\mu\text{-}Cl)_2(DME)_4][AlEtCl_3]_2$ and (b) $[Mg_2(\mu\text{-}Cl)_2(DME)_4][AlCl_4]_2$. Mg atoms are shown in blue, Cl atoms in green, O atoms in red, Al atoms in ivory, and carbon atoms in grey. The OLEX plot at 30% thermal probability ellipsoids. Hydrogen atoms are not shown for clarity. Molecular structures of (a) $[Mg_2(\mu\text{-}Cl)_2(DME)_4][AlEtCl_3]_2$ and (b) $[Mg_2(\mu\text{-}Cl)_2(DME)_4][AlCl_4]_2$ (Mg, blue; l Cl, green; Al, grey; C, color). The OLEX plot at 30% thermal probability ellipsoids. Hydrogen atoms are not shown for clarity. Pertinent bond angles and lengths for (a): Cl(1)–Mg(1)–Cl(2): 89.24°, Cl(1)–Mg(2)–Cl(2): 88.46°, Mg(1)–Cl(1) and Mg(1)–Cl(2): 2.446 Å, and Mg(2)–Cl(1) and Mg(2)–Cl(2): 2.463 Å. Mg(1)–O bonds have identical lengths of 2.096 Å, Mg(2)–$O_{equatorial}$: 2.112 Å, Mg(2)–O_{axial}: 2.075 Å, Al–C(11): 1.970 Å, and Al–Cl average bond length of 2.125 Å. Pertinent bond angles and lengths for (b): Cl(1)–Mg(1)–Cl(2): 88.00°, Cl(1)–Mg(2)–Cl(2): 87.41°, Mg(1)–Cl(1): 2.425 Å, Mg(1)–Cl(2): 2.456 Å, Mg(2)–Cl(1): 2.472 Å, Mg(2)–Cl(2): 2.435 Å. Mg(1)–O average length of 2.099 Å, Mg(2)–O(7): 2.112 Å, Mg(2)–O(6) 2.101 Å, and Al–Cl average bond length of 2.131 Å.

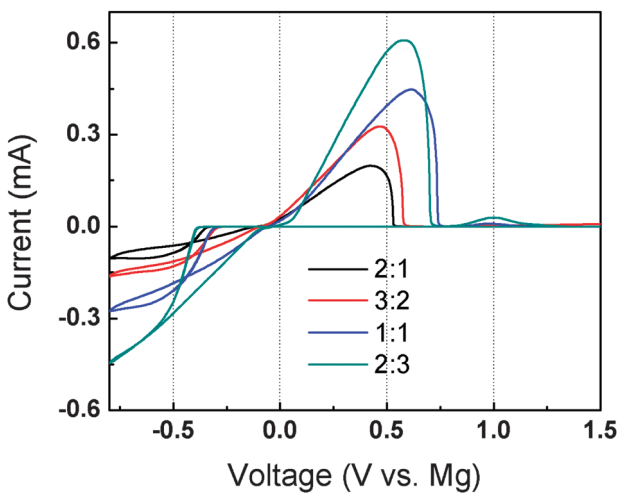

Fig. 3 CV (2nd cycle) of 0.4 M $MgCl_2$ electrolyte solutions synthesized in DME with different ratios of $AlEtCl_2$ as indicated (the ratios refer to the molar ratio between $MgCl_2$ and $AlEtCl_2$). These data were measured on a 1 mm Pt working electrode at a scan rate of 20 mV s^{-1}.

Table 2 Electrochemical properties of electrolytes synthesized using 0.4 M $MgCl_2$ and desired $AlEtCl_2$ in different solvents as indicated. These data were obtained based on CV experiments with Pt working electrodes (1 mm) at 20 mV s^{-1}

Solvent	Overpotential for Mg deposition (mV)	Coulombic efficiency (%)	Conductivity (mS cm^{-1})
0.4 M $MgCl_2$ + 0.2 M $AlEtCl_2$/DME	216	95	2.10
0.4 M $MgCl_2$ + 0.27 M $AlEtCl_2$/DME	202	95	2.72
0.4 M $MgCl_2$ + 0.4 M $AlEtCl_2$//DME	220	95	3.90
0.4 M $MgCl_2$ + 0.6 M $AlEtCl_2$//DME	360	85	4.32
0.8 M $MgCl_2$ + 0.8 M $AlEtCl_2$/DME	209	95	6.72

using a Pt electrode at 20 mV s^{-1}, and Table 2 compares their activities for Mg deposition and ionic conductivity. It was observed that electrochemical properties of these electrolytes had strong dependence on the precursor ratios. In particular, both ionic conductivity and Mg deposition current density increased noticeably with the increase of $AlEtCl_2$ concentration. The solutions synthesized with low concentrations of $AlEtCl_2$ ($\leq$0.4 M) had similar overpotential ($\sim$200 mV) and coulombic efficiency ($\sim$95%) for Mg deposition whereas the solution with excess $AlEtCl_2$ (0.6 M) had noticeably higher overpotential and lower coulombic efficiency. Additionally, a small anodic peak at $\sim$1.0 V was observed when the concentration of $AlEtCl_2$ exceeds 0.4 M and will be discussed below. If we assume that ionic species in this electrolyte were mostly $[Mg_2(\mu\text{-}Cl)_2(DME)_4]^{2+}$ cations and $AlEtCl_3^-$ anions, the observed higher ionic conductivity and Mg deposition activity with the increased concentration of $AlEtCl_2$ suggest that more ionic species are generated. This assumption is reasonable because compared with the case in THF, formation of species such as $MgCl^+$ and $Mg_2Cl_3^+$ is not favored thermodynamically in DME due to difficulties in fulfilling a coordination number of 6.[26,35]

To better explain the obtained data, we propose that the reaction for our experiments was under dynamic equilibrium and did not completely convert to the dimer species with stoichiometric precursors. Even though it is not clear what the limiting step for the reaction is, it is evident that increasing the concentration of $AlEtCl_2$ will drive the reaction and result in higher yields of the dimer cation. To gain more insight, we characterized these electrolytes by ^{27}Al NMR (Fig. 4). The ^{27}Al NMR spectrum is very sensitive to the symmetry of the molecule and the nature of the ligands and therefore ^{27}Al NMR is a useful technique to identify Al species. Three main ^{27}Al resonances were observed from these electrolytes and they can be assigned based on the results from standard solutions as well as from the literature.[26,36] The peaks at chemical shifts of $\sim$24.5 ppm and $\sim$128 ppm can be assigned to the precursor compound $AlEtCl_2$.[37] The peak at $\sim$103.0 ppm could be assigned to $AlCl_4^-$,[13,35] which is believed to originate from ligand exchange of $AlEtCl_3^-$. The broad peak at $\sim$127.9 ppm can be assigned to $AlEtCl_3^-$.[38] Among species presented, the resonance attributed to $AlEtCl_2$ (at 24.5 ppm) is particularly meaningful for understanding the reaction. When the ratio between $MgCl_2$ and $AlEtCl_2$ was 2 : 1 no residual $AlEtCl_2$ was observed. Trace amounts of this species were observed for the 1 : 1 combination and with a considerable amount present when the ratio was 1 : 1.5. These comparisons suggest that with the 1 : 1 ratio the reaction will not go to completion and some unreacted $AlEtCl_2$, as well as some solvated $MgCl_2$, were still present in the solution. Excess $MgCl_2$ is needed for complete reaction of $AlEtCl_2$ and excess $AlEtCl_2$ will likewise be required for complete conversion of $MgCl_2$ to the dimer cation complex.

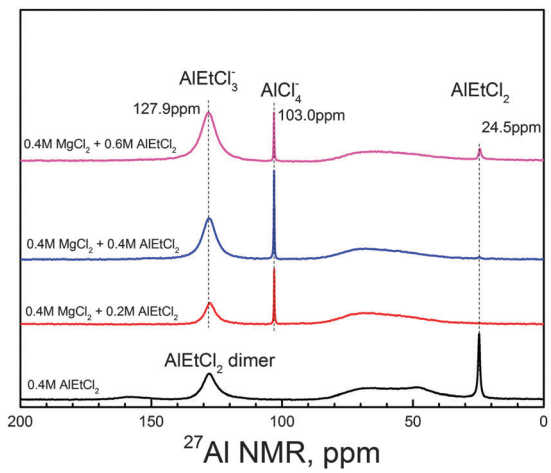

Fig. 4 ^{27}Al NMR spectra of different solutions as indicated.

The electrochemistry and spectroscopy results confirm that the reaction between $MgCl_2$ and $AlEtCl_2$ will not convert them to a dimer cation complex completely and the degree of conversion will be thermodynamically limited even at elevated temperature (60 °C as used in this study). This fact is important for understanding the properties of electrolytes, as the species present in the electrolyte could have pronounced effects on the cycling behavior of batteries. For example, the solution with excess $AlEtCl_2$ (0.6 M, Table 2) exhibited a noticeably higher overpotential and a lower coulombic efficiency along with a small cathodic peak at $\sim$1.0 V. This peak is at a position similar to the oxidization of the Al metal and therefore suggest the formation of Al species in this electrolyte.[16] These results imply that residual $AlEtCl_2$ could substantially affect the electrochemical activity and stability of the electrolyte and its concentration should be minimized through controlling the concentration of $MgCl_2$.

The above results clearly suggest that the dimer $[Mg_2(\mu\text{-}Cl)_2\text{-}(DME)_4]^{2+}$ complex is present in electrolytes synthesized using $MgCl_2$–$AlEtCl_2$ in DME, and it is logical to study whether this complex is generally present in DME-based electrolytes. To address this question, we synthesized and analyzed two additional sets of solutions by reacting 0.4 M $MgCl_2$ with either 0.4 M $AlCl_3$ or 0.4 M $Mg(TFSI)_2$ in DME. Single crystal XRD analysis performed on the $MgCl_2$–$AlCl_3$/DME electrolyte revealed that the ionic pair was indeed $[Mg_2(\mu\text{-}Cl)_2(DME)_4][AlCl_4]_2$

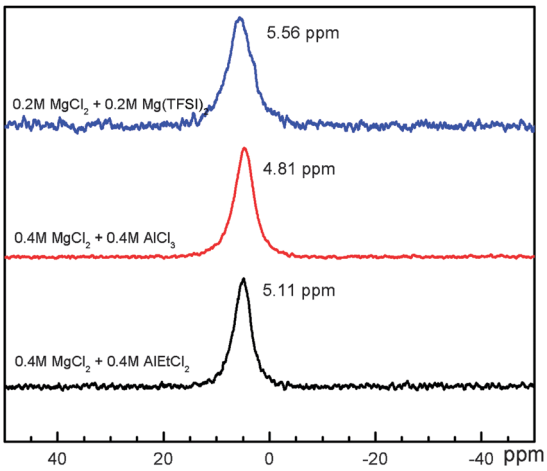

Fig. 5 ^{25}Mg NMR spectra of different electrolytes synthesized in DME.

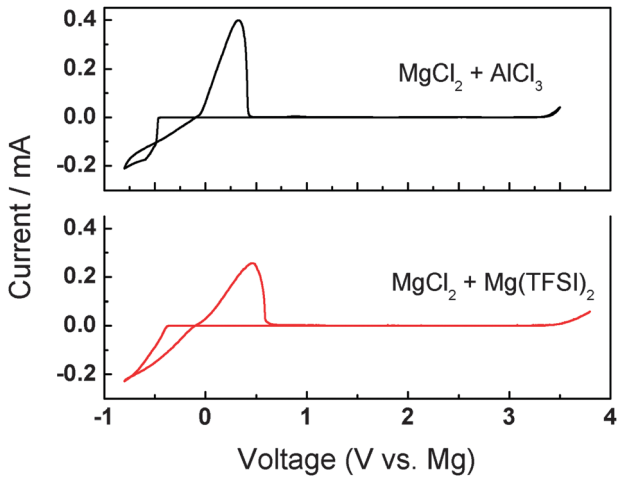

Fig. 6 CV (2nd cycle) of electrolytes synthesized in DME by reacting 0.4 M $MgCl_2$ with 0.4 M $AlCl_3$ or 0.4 M $Mg(TFSI)_2$ as indicated, measured on a Pt working electrode at a scan rate of 20 mV s^{-1}.

(Fig. 2b and Tables S7–S12, ESI†). We then performed ^{25}Mg NMR analysis on these three solutions, since multinuclear NMR spectroscopy has been demonstrated as a suitable technique for analyzing the chemical structure of complex Mg electrolyte solutions.[26,35] Chemical shifts of Mg ions for these three electrolytes were similar and were all around ~5 ppm (Fig. 5). Given the high sensitivity of Mg chemical shifts in the chemical environment, we believe that the same cation complex was formed in each of these electrolytes.

Fig. 6 compares the electrochemical activities of these two electrolytes (see Fig. 1 and 3 for $MgCl_2$–$AlEtCl_2$/DME electrolytes). It was found that both of them had good activity for Mg deposition/dissolution, and electrochemical windows wider than the $MgCl_2$–$AlEtCl_2$/DME electrolyte due to differences in anions. The $MgCl_2$–$AlCl_3$/DME electrolyte had an overpotential of ~200 mV, a coulombic efficiency of 95% and an anodic stability of ~3.4 V, whereas the $MgCl_2$–$Mg(TFSI)_2$/DME electrolyte had an overpotential of ~400 mV, an efficiency of ~80% and an anodic stability of ~3.5 V. The comparison of these results with the $MgCl_2$–$AlEtCl_2$/DME electrolyte suggests that the chemistry of anions has strong influences on the behavior of electrolytes. It should be noted, however, that other factors (such as impurities and precursor compound ratios) might also contribute to the differences in the measured performance results. Further studies on the mechanistic understanding of these electrolytes consisting of $[Mg_2(\mu\text{-}Cl)_2(DME)_4]$ using approaches similar to the study of the $MgCl_2$–$AlEtCl_2$/DME electrolyte could further optimize their activities for Mg deposition.

On the basis of the above results, the pathways for electrolyte synthesis in DME were rationalized as dehalodimerization of $MgCl_2$ and are shown in Schemes 1 and 2. The dehalodimerization process involves mono-Cl transfer from $MgCl_2$ to some chemical species that can be generally termed chloride ion acceptors, and the overall reaction was driven thermodynamically by the ability of the acceptor to abstract one Cl^- off $MgCl_2$ and/or formation of the more stable dimer species. Overall, it has been recognized that the solvated Mg^{2+} ion has a six-coordinated, octahedral structure. The structure of solvated $MgCl_2$ in THF has been reported as *trans*-$MgCl_2(THF)_4$.[13] In analogy with THF, we propose that the most feasible structure of solvated $MgCl_2$ in DME is *trans*-$MgCl_2(DME)_2$ as shown in the scheme. During the reaction, one equivalent of *trans*-$MgCl_2(DME)_2$ transfers one equivalent of chloride ion to the acceptor through a Cl transfer pathway. The chloride ion acceptor could be a Lewis acid compound, such as $AlEtCl_2$ and $AlCl_3$, or a Mg compound that is solvable in DME, such as $Mg(TFSI)_2$. The mechanism of mono-Cl transfer (reaction a) for the reaction of $MgCl_2$ and a Lewis acid compound is straightforward as Lewis acid is a strong electron acceptor. The chloride abstraction results in the formation of metastable $[MgCl(DME)_2]^+$ cations, which then undergo a self-dimerization process (reaction b) to form thermodynamically more stable $[Mg_2(\mu\text{-}Cl)_2(DME)_4]^{2+}$ dimer cations.

The reaction of $MgCl_2$ and $Mg(TFSI)_2$, however, is not straightforward and can be understood as follows (Scheme 2). $TFSI^-$ is a bulky non-coordinating anion and does not involve

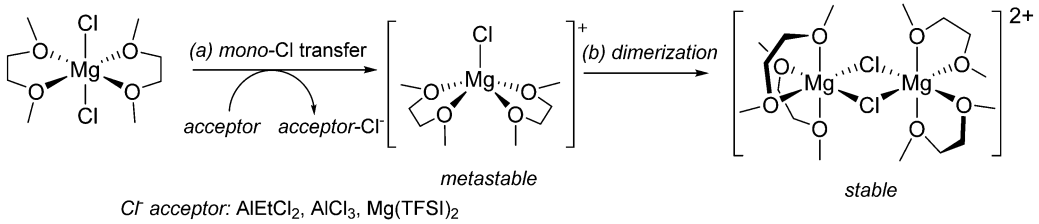

Scheme 1 Proposed reaction path to $[Mg_2(\mu\text{-}Cl)_2DME_4]^{2+}$ *via* mono-Cl transfer.

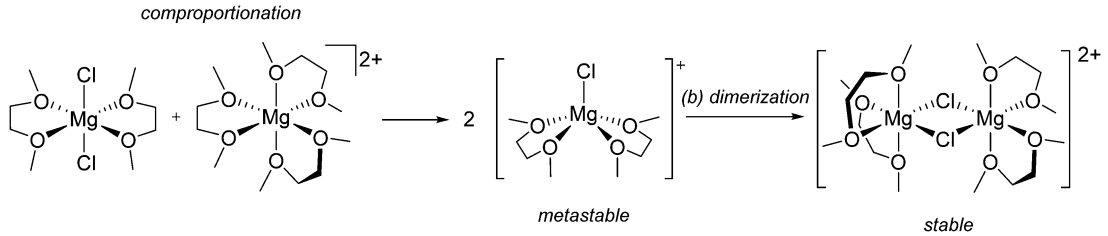

Scheme 2 Proposed reaction path to $[Mg_2(\mu\text{-}Cl)_2DME_4]^{2+}$ *via* comproportionation.

the first coordination shell of DME-solvated Mg^{2+}, which should have the structure of $[Mg^{2+}(DME)_3](TFSI)_2$ based on the ^{25}Mg NMR measurement (−0.94 ppm, Fig. S1, ESI†).[39] The stabilization of the highly charged cation $[Mg(DME)_3]^{2+}$ from a strong anionic ligand, such as Cl^-, would be sufficient enough to abstract a Cl^- ion from the solvated $MgCl_2$. This results in an overall comproportionation to again afford metastable $[MgCl(DME)_2]^+$ cations from Cl^- transfer. After dimerization, it is possible that there is dynamic equilibrium between the species of $MgCl_2(DME)_2$, $[MgCl(DME)_2]^+$, and $[Mg_2(\mu\text{-}Cl)_2(DME)_4]^{2+}$ and their ratio is determined thermodynamically. In comparison with typical electrolytes synthesis in THF that involved transmetalation reaction between organomagnesium and Lewis acids that results in the generation of a complex mixture of species with various moieties,[10,40] the present synthesis is straightforward and cleaner with minimal side-reaction products. In fact, the comparison of the Raman spectra of the $[Mg_2(\mu\text{-}Cl)_2(DME)_4][AlEtCl_3]_2$ solid crystals and the electrolyte solutions reveals that no Mg-related peaks other than the dimer species were observed (Fig. S2, ESI†). The present clean electrolyte solutions with well-defined solution chemistry could have particular significance for the understanding and design of Mg cathode research.[31]

The Mg metal deposited from the $MgCl_2$–$AlEtCl_2$/DME electrolyte was analyzed by XRD, SEM and EDX. The deposition rate was 1 mA cm^{-2} and a piece of Pt foil was used as the deposition substrate. Fig. 7a shows the XRD diffraction pattern collected

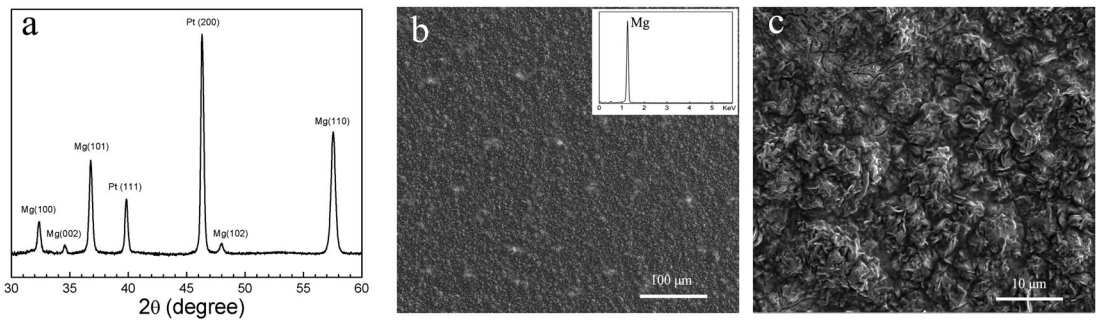

Fig. 7 (a) XRD diffraction patterns of Mg deposited on Pt and (b and c) the typical SEM image of the deposited Mg showing non-dendritic morphology. The inset in (b) is the EDS spectrum showing 100% Mg deposition.

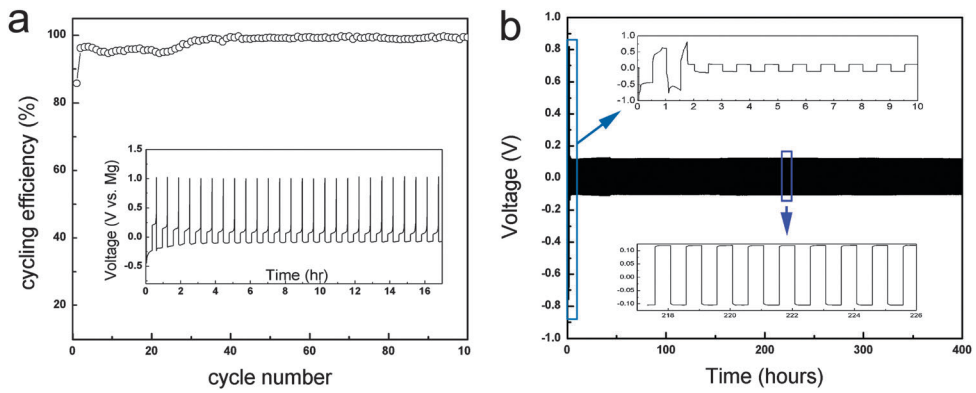

Fig. 8 Cycling behavior of the 0.4 M $MgCl_2$–$AlEtCl_2$/DME electrolyte (a) coulombic efficiency of coin cells assembled with a Cu disk positive electrode and a Mg disk negative electrode, measured at a current density of 0.5 mA cm^{-2}. The inset is the initial 25 cycles of Mg deposition/stripping; (b) voltage profile of Mg–Mg symmetric cells tested with a high current density of 8.0 mA cm^{-2} for 400 cycles, 30 min for charging and 30 min for discharging, both the anode and cathode disk are Mg metals.

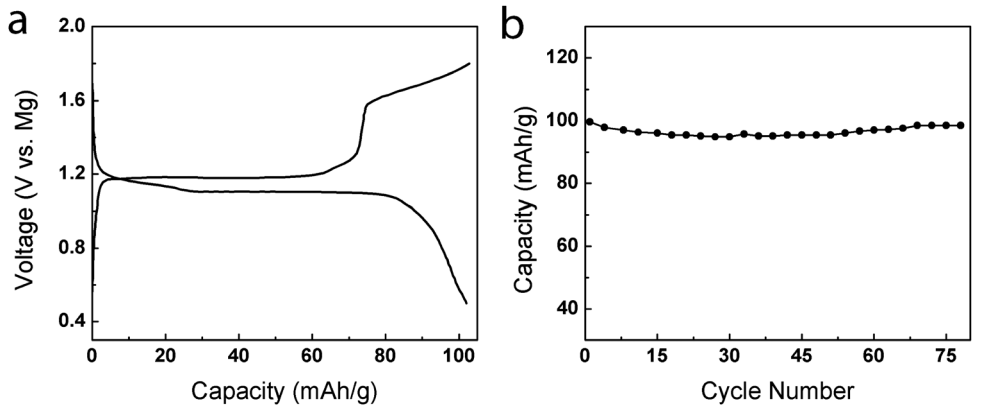

Fig. 9 Galvanostatic cycling of the Mo_6S_8 cathode in the electrolyte prepared by 0.4 M $MgCl_2$–$AlEtCl_2$ in DME at a rate of C/10: (a) the typical charge–discharge profile and (b) cyclic stability for 75 cycles. The battery tests were conducted at room temperature.

from the sample, suggesting successful deposition of Mg metals. Fig. 7b and c show the SEM images, revealing that the deposited Mg metal is smooth, uniform and free of dendritic structures. The deposited Mg grains are in rock shape with the sizes of 5–10 μm. Such uniform Mg deposition is very important for practical uses. EDS measurements (Fig. 7b, inset) further confirmed pure magnesium without impurities.

The Mg deposition and stripping behavior of the 0.4 M $MgCl_2$–$AlEtCl_2$/DME electrolyte were further evaluated *via* chronopotentiometry using coin cells, which contains a Cu positive electrode and an Mg negative electrode. The coulombic efficiency (to a final stripping potential of 1.0 V) for the first cycle was ~85% but quickly increased to >95% for the second and subsequent cycles (Fig. 8a). Overall, the stabilized cycling efficiency was ~99%. Despite the high initial overpotential for activation, the cycling for over hundreds of cycles afforded an average cell overpotential of ~100 mV. In another set of experiments to evaluate this electrolyte, we assembled Mg//Mg symmetric coin cells and tested these cells *via* chronopotentiometry at a high current density of 8.0 mA cm^{-2}, with the charging and discharging time both set at 30 min. Fig. 8b shows typical voltage profiles for 400 cycles. A similarly high overpotential of ~600 mV was observed for the initial few cycles (~3 cycles) but the overpotential for stabilized cycling was ~100 mV and was very stable, with no obvious voltage spike or appreciable increase over continuous cycles.

To confirm the compatibility of electrolytes containing the $[Mg_2(\mu\text{-}Cl)_2(DME)_4]^{2+}$ complex with Mg^{2+} ion intercalation cathodes, prototype coin cells were assembled using Mg disk anodes and Chevrel phase Mo_6S_8 cathodes and were tested. The typical charge–discharge profiles at a rate of C/10 are shown in Fig. 9a. The typical reversible capacity was ~100 mA h g^{-1} and the voltage profile is comparable to those observed when cycling in the APC electrolytes (Fig. 9a).[5] The cycling tests suggest minimal capacity fade upon cycling (Fig. 9b). The well-defined charge–discharge profiles suggest a highly reversible intercalating behavior of Mg^{2+} ions in the electrolyte into Mo_6S_8 cathodes. These results clearly suggest that a $[Mg_2(\mu\text{-}Cl)_2(DME)_4]^{2+}$ complex based electrolyte can be incorporated into rechargeable Mg batteries.

Conclusions

In summary, we established the formulation and first identification of the unique cation complex $[Mg_2(\mu\text{-}Cl)_2(DME)_4]^{2+}$ for highly active Mg electrolytes. This cation complex can be formulated in DME by dehalodimerization of non-nucleophilic $MgCl_2$ through reacting with either a Mg salt $Mg(TFSI)_2$ or a Lewis acid salt ($AlEtCl_2$ or $AlCl_3$) and its structure was extensively studied using single-crystal XRD, Raman and NMR characterization methods. The feasibility of these electrolytes for practical Mg batteries was evidenced by their outstanding Mg deposition activity and reversibility (up to 100% stable cycling efficiency), high anodic stability (up to 3.5 V) and ionic conductivity. The new active species identified here and its synthesis and understanding could provide new approaches for rational formulation of Mg electrolytes and design of high energy density magnesium batteries.

Conflicts of interest

The authors declare no competing financial interest.

Acknowledgements

We would like to gratefully acknowledge the support from the U.S. Department of Energy (DOE) Office of Electricity Delivery and Energy Reliability under Contract No. 57558 and the Laboratory-Directed Research and Development Program of Pacific Northwest National Laboratory (PNNL). NMR, Raman, and SEM characterization methods were performed in the Environmental Molecular Sciences Laboratory, a national scientific user facility sponsored by DOE's Office of Biological and Environmental Research, located at PNNL. PNNL is a multiprogram laboratory operated by Battelle Memorial Institute for the DOE under Contract DE-AC05-76RL01830.

References

1 D. Aurbach, Z. Lu, A. Schechter, Y. Gofer, H. Gizbar, R. Turgeman, Y. Cohen, M. Moshkovich and E. Levi, *Nature*, 2000, **407**, 724–727.

2 H. D. Yoo, I. Shterenberg, Y. Gofer, G. Gershinsky, N. Pour and D. Aurbach, *Energy Environ. Sci.*, 2013, **6**, 2265–2279.
3 P. Saha, M. K. Datta, O. I. Velikokhatnyi, A. Manivannan, D. Alman and P. N. Kumta, *Prog. Mater. Sci.*, 2014, **66**, 1–86.
4 Y. W. Cheng, Y. Y. Shao, J. G. Zhang, V. L. Sprenkle, J. Liu and G. S. Li, *Chem. Commun.*, 2014, **50**, 9644–9646.
5 Y. Cheng, L. R. Parent, Y. Shao, C. Wang, V. L. Sprenkle, G. Li and J. Liu, *Chem. Mater.*, 2014, **26**, 4904–4907.
6 Y. L. Liang, R. J. Feng, S. Q. Yang, H. Ma, J. Liang and J. Chen, *Adv. Mater.*, 2011, **23**, 640–643.
7 Y. N. NuLi, Y. P. Zheng, F. Wang, J. Yang, A. I. Minett, J. L. Wang and J. Chen, *Electrochem. Commun.*, 2011, **13**, 1143–1146.
8 R. G. Zhang, X. Q. Yu, K. W. Nam, C. Ling, T. S. Arthur, W. Song, A. M. Knapp, S. N. Ehrlich, X. Q. Yang and M. Matsui, *Electrochem. Commun.*, 2012, **23**, 110–113.
9 Y. Y. Shao, T. B. Liu, G. S. Li, M. Gu, Z. M. Nie, M. Engelhard, J. Xiao, D. P. Lv, C. M. Wang, J. G. Zhang and J. Liu, *Sci. Rep.*, 2013, **3**, 3130.
10 N. Pour, Y. Gofer, D. T. Major and D. Aurbach, *J. Am. Chem. Soc.*, 2011, **133**, 6270–6278.
11 J. Muldoon, C. B. Bucur, A. G. Oliver, T. Sugimoto, M. Matsui, H. S. Kim, G. D. Allred, J. Zajicek and Y. Kotani, *Energy Environ. Sci.*, 2012, **5**, 5941–5950.
12 Y. S. Guo, F. Zhang, J. Yang, F. F. Wang, Y. N. NuLi and S. I. Hirano, *Energy Environ. Sci.*, 2012, **5**, 9100–9106.
13 T. B. Liu, Y. Y. Shao, G. S. Li, M. Gu, J. Z. Hu, S. C. Xu, Z. M. Nie, X. L. Chen, C. M. Wang and J. Liu, *J. Mater. Chem. A*, 2014, **2**, 3430–3438.
14 Z. Zhao-Karger, J. E. Mueller, X. Y. Zhao, O. Fuhr, T. Jacob and M. Fichtner, *RSC Adv.*, 2014, **4**, 26924–26927.
15 R. E. Doe, R. Han, J. Hwang, A. J. Gmitter, I. Shterenberg, H. D. Yoo, N. Pour and D. Aurbach, *Chem. Commun.*, 2014, **50**, 243–245.
16 S. Yagi, A. Tanaka, Y. Ichikawa, T. Ichitsubo and E. Matsubara, *J. Electrochem. Soc.*, 2013, **160**, C83–C88.
17 Y. W. Cheng, T. B. Liu, Y. Y. Shao, M. H. Engelhard, J. Liu and G. S. Li, *J. Mater. Chem. A*, 2014, **2**, 2473–2477.
18 D. P. Lv, T. Xu, P. Saha, M. K. Datta, M. L. Gordin, A. Manivannan, P. N. Kumta and D. H. Wang, *J. Electrochem. Soc.*, 2013, **160**, A351–A355.
19 N. Singh, T. S. Arthur, C. Ling, M. Matsui and F. Mizuno, *Chem. Commun.*, 2013, **49**, 149–151.
20 Y. Y. Shao, M. Gu, X. L. Li, Z. M. Nie, P. J. Zuo, G. S. Li, T. B. Liu, J. Xiao, Y. W. Cheng, C. M. Wang, J. G. Zhang and J. Liu, *Nano Lett.*, 2014, **14**, 255–260.
21 T. S. Arthur, N. Singh and M. Matsui, *Electrochem. Commun.*, 2012, **16**, 103–106.
22 J. M. Tarascon and M. Armand, *Nature*, 2001, **414**, 359–367.
23 M. C. Kroon, W. Buijs, C. J. Peters and G. J. Witkamp, *Green Chem.*, 2006, **8**, 241–245.
24 Z. Lu, A. Schechter, M. Moshkovich and D. Aurbach, *J. Electroanal. Chem.*, 1999, **466**, 203–217.
25 C. Liao, B. K. Guo, D. E. Jiang, R. Custelcean, S. M. Mahurin, X. G. Sun and S. Dai, *J. Mater. Chem. A*, 2014, **2**, 581–584.
26 O. Mizrahi, N. Amir, E. Pollak, O. Chusid, V. Marks, H. Gottlieb, L. Larush, E. Zinigrad and D. Aurbach, *J. Electrochem. Soc.*, 2008, **155**, A103–A109.
27 T. D. Gregory, R. J. Hoffman and R. C. Winterton, *J. Electrochem. Soc.*, 1990, **137**, 775–780.
28 D. Lv, D. Tang, Y. Duan, M. L. Gordin, F. Dai, P. Zhu, J. Song, A. Manivannan and D. Wang, *J. Mater. Chem. A*, 2014, **2**, 15488–15494.
29 D. Aurbach, A. Schechter, M. Moshkovich and Y. Cohen, *J. Electrochem. Soc.*, 2001, **148**, A1004–A1014.
30 F. F. Wang, Y. S. Guo, J. Yang, Y. Nuli and S. Hirano, *Chem. Commun.*, 2012, **48**, 10763–10765.
31 H. S. Kim, T. S. Arthur, G. D. Allred, J. Zajicek, J. G. Newman, A. E. Rodnyansky, A. G. Oliver, W. C. Boggess and J. Muldoon, *Nat. Commun.*, 2011, **2**, 427.
32 R. E. Doe, G. H. Lan, R. E. Jilek and J. H. Hwang, US20130252114, 2013.
33 S. Y. Ha, Y. W. Lee, S. W. Woo, B. Koo, J. S. Kim, J. Cho, K. T. Lee and N. S. Choi, *ACS Appl. Mater. Interfaces*, 2014, **6**, 4063–4073.
34 J. Muldoon and C. B. Bucur, US8722242 B2, 2011.
35 Y. Gofer, O. Chusid, H. Gizbar, Y. Viestfrid, H. E. Gottlieb, V. Marks and D. Aurbach, *Electrochem. Solid-State Lett.*, 2006, **9**, A257–A260.
36 M. C. Lefebvre and B. E. Conway, *J. Electroanal. Chem.*, 1998, **448**, 217–227.
37 A. G. Potapov, V. V. Terskikh, G. D. Bukatov and V. A. Zakharov, *J. Mol. Catal. A: Chem.*, 2000, **158**, 457–460.
38 C. E. Keller and W. R. Carper, *Inorg. Chim. Acta*, 1993, **210**, 203–208.
39 P. H. Heubel and A. I. Popov, *J. Solution Chem.*, 1979, **8**, 283–291.
40 H. Gizbar, Y. Vestfrid, O. Chusid, Y. Gofer, H. E. Gottlieb, V. Marks and D. Aurbach, *Organometallics*, 2004, **23**, 3826–3831.

